1 Dynamic Modeling

The model of the AMB-flexible rotor test rig is shown in the Figure 1(**also in the file *pictures/AMB-flexible rotor_system.png***), and the modeling prototype is based on the high-pressure rotor section of a certain gas turbine. The test rig consists of a slender flexible rotor with a length of 1060 mm and a diameter of 20 mm. Three rigid disks, labeled B1–B3, are mounted on the shaft and positioned on either side of the magnetic bearings to simulate the mass distribution of the blade disks in the high-pressure rotor of the prototype. To enhance the mechanical strength of the shaft at the nodes where the magnetic bearings act, and to prevent localized fatigue or cracking during high-speed rotation, the shaft is thickened at the two magnetic bearing action points by adding journal sections A1 and A2. The mass and rotational inertia information for each component of the flexible rotor system is listed in Table 1.

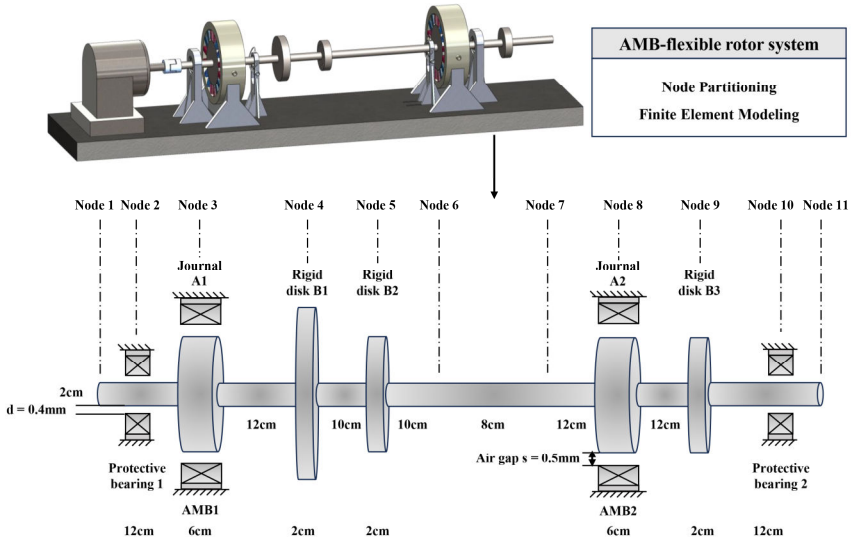

Figure 1 Schematic diagram of the active magnetic bearing-flexible rotor system.

Table 1 Parameters of the flexible rotor shaft and disks.

Component	Mass (kg)	Polar Moment of Inertia (kg·m²)	Equatorial Moment of Inertia (kg·m²)
Journal A1	5.1437	0.00926	0.00617
Journal A2	5.1437	0.00926	0.00617
Disk B1	1.7146	0.00309	0.00160
Disk B2	0.7620	0.00061	0.00033
Disk B3	0.7620	0.00061	0.00033

The dynamic equation for the flexible rotor system established using the finite element method in the appendix is

$$\mathbf{M}\ddot{\mathbf{X}} + (\mathbf{C} - \omega\mathbf{G})\dot{\mathbf{X}} + \mathbf{K}\mathbf{X} = \mathbf{F}_g + \mathbf{F}_m + \mathbf{F}_u. \quad (1)$$

In the equation, $\boldsymbol{M}$, $\boldsymbol{C}$, $\boldsymbol{G}$, and $\boldsymbol{K}$ represent the mass matrix, damping matrix, gyroscopic matrix, and stiffness matrix, respectively. $\boldsymbol{F_g}$, $\boldsymbol{F_m}$, $\boldsymbol{F_u}$, and $\boldsymbol{F_d}$ denote the gravitational force, magnetic bearing force, unbalanced force, and external disturbance, respectively.

Since the initial system matrix is too large to compute efficiently, we performed eigenvalue-based order reduction and selected the first four system modes for simplification. **To facilitate readers in reproducing our work, we have provided the reduced 16×16-dimensional *M*, *C*, *G*, and *K* matrices in the GitHub repository(AMB-flexible rotor system parameters.xlsx).**

Assuming the equivalent stiffness coefficients of the magnetic bearings are constants, the variation of the natural frequencies of the flexible rotor under different rotational speeds is calculated, and the Campbell diagram of the flexible rotor is plotted, as shown in the Figure 2(**also in the file *pictures/campbell diagram.png***). From the diagram, it can be observed that the first-order flexible mode critical speed of the modeled flexible rotor is 3257 rpm. For industrial applications, a rotational speed exceeding 70% of the critical speed can be regarded as flexible, and the operating conditions in this study primarily exceed the critical speed. Therefore, the rotor can be considered flexible.

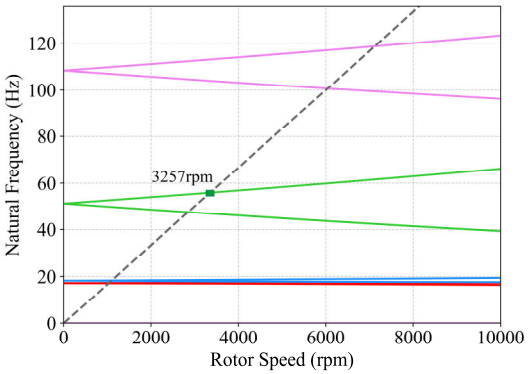

Figure 2 Campbell diagram of the flexible rotor system.

2 AMBs-Flexible Rotor State-Space Model

Let 4×16 matrix $\boldsymbol{T_a}$ be the transformation matrix that maps the generalized displacement vector of the flexible rotor to the AMB journal displacement vector. The dynamic equation (1) can then be reformulated into a state-space model.

$$\begin{aligned}\begin{bmatrix}\dot{x}\\ \ddot{x}\end{bmatrix}&=\begin{bmatrix}\mathbf{0} & \mathbf{I}\\ -\mathbf{M}^{-1}\mathbf{K} & -\mathbf{M}^{-1}(\mathbf{C}-\Omega\mathbf{G})\end{bmatrix}\begin{bmatrix}x\\ \dot{x}\end{bmatrix}+\\ &\begin{bmatrix}\mathbf{0}\\ \mathbf{M}^{-1}\mathbf{T}\mathbf{a}^{\mathrm{T}}\end{bmatrix}\mathbf{F}_{\mathbf{m}}(x,u)+\begin{bmatrix}\mathbf{0}\\ \mathbf{M}^{-1}\end{bmatrix}(\mathbf{F}_{\mathbf{u}}+\mathbf{F}_{\mathbf{g}}),\\ y&=\begin{bmatrix}\mathbf{T}\mathbf{a} & \mathbf{0}\end{bmatrix}\begin{bmatrix}x\\ \dot{x}\end{bmatrix}.\end{aligned}\tag{2}$$

In our study, the continuous-time system was discretized using a zero-order holder with a sampling time of 5×10^{-5} seconds. The subsequent tests were all based on the discrete model. The state-space representation is discretized as

$$\begin{aligned}&\mathbf{X}(\mathbf{k}+\mathbf{1})=\mathbf{A}_{\mathbf{d}}\mathbf{X}(\mathbf{k})+\mathbf{F}(\mathbf{X}(\mathbf{k}),\mathbf{u}(\mathbf{k})),\\ &\mathbf{Y}=\mathbf{C}_{\mathbf{d}}\mathbf{X}(\mathbf{k}).\end{aligned}\tag{3}$$

where u represents the control current i. At this point, the system becomes a nonlinear system, further increasing the difficulty in observing the states of the flexible rotor.

Appendix: Finite Element Modeling

A.1 Flexible Rotor Shaft Modeling

The shaft segment serves as the fundamental unit of flexible rotor shafts. Each segment can be modeled as a homogeneous uniform-cross-section beam element, where the motion is characterized by displacement vectors at both end nodes.

Mathematically, each beam element contains two nodes (denoted k and k+1) with four degrees of freedom (DOF) per node: two translational displacements (x, y) and two rotational angles. Consequently, the Timoshenko beam element requires eight DOF for complete kinematic description

$$\begin{aligned}q_s^k&=\begin{bmatrix}x_1 & \theta_{x1} & y_2 & \theta_{y2}\end{bmatrix}^{\mathrm{T}},\\ q_s^{k+1}&=\begin{bmatrix}x_2 & \theta_{x2} & y_1 & \theta_{y1}\end{bmatrix}^{\mathrm{T}}.\end{aligned}\tag{4}$$

where q_s^k denotes the generalized displacements of the beam element at the k-th node, with x and y representing translational displacements and θ indicating rotational angles. The dynamic equations are then derived using Lagrange's equations.

$$\begin{aligned}\mathbf{M}_{\mathbf{s}}\ddot{q}_s^k+\omega\mathbf{J}_{\mathbf{s}}\dot{q}_s^{k+1}+\mathbf{K}_{\mathbf{s}}\dot{q}_s^k&=F_s^x,\\ \mathbf{M}_{\mathbf{s}}\ddot{q}_s^{k+1}-\omega\mathbf{J}_{\mathbf{s}}\dot{q}_s^k+\mathbf{K}_{\mathbf{s}}\dot{q}_s^{k+1}&=F_s^y.\end{aligned}\tag{5}$$

In the above Equation (5), $\boldsymbol{M_s}$, $\boldsymbol{J_s}$, and $\boldsymbol{K_s}$ denote the mass matrix, inertia matrix, and stiffness matrix of the beam element respectively. ω represents the rotational speed, and $\boldsymbol{F_s}$ indicates the resultant external force acting on the beam element nodes.

A.2 Rigid Disk Modeling

In the flexible rotor system, disks B1, B2, B3 and thickened journals A1, A2 are modeled as rigid disks. This implies that only kinetic energy is considered in the energy calculation for these components, while strain energy is neglected. The motion of each disk is characterized by four degrees of freedom: horizontal displacement x, vertical displacement y, and rotational angles θ_x, θ_y about the x- and y-axes respectively. The generalized displacements in the x- and y-directions are defined as

$$\begin{aligned}q_d^x&=\begin{bmatrix}x & \theta_x\end{bmatrix}^{\mathrm{T}},\\ q_d^y&=\begin{bmatrix}y & \theta_y\end{bmatrix}^{\mathrm{T}}.\end{aligned}\tag{6}$$

The dynamic equations of the rigid disks can be derived using Lagrange's equation.

$$\begin{aligned}\mathbf{M}_{\mathbf{d}}\ddot{q}_d^x+\omega\mathbf{J}_{\mathbf{d}}\dot{q}_d^y&=F_d^x,\\ \mathbf{M}_{\mathbf{d}}\ddot{q}_d^x+\omega\mathbf{J}_{\mathbf{d}}\dot{q}_d^y&=F_d^x.\end{aligned}\tag{7}$$

In the equation, $\boldsymbol{M_d}$ denotes the mass matrix of the disk, $\boldsymbol{J_d}$ represents the inertia matrix of the disk, and F_d corresponds to the generalized external force acting on the disk.

A.3 Unbalance Force and Gravity Modeling

The modeling of unbalance forces requires experimental measurement of imbalance magnitudes in flexible rotor systems. During manufacturing, flexible rotors inevitably develop mass unevenness, causing the center of mass to deviate from the geometric center. This mass imbalance generates centrifugal forces during rotation, inducing unbalance vibrations. For node k, given the unbalanced mass m_k and eccentricity e_k between the mass center and geometric center of the rigid disk, the unbalance force at node k can be expressed as

$$F_u^k=\begin{bmatrix}f_x\\ f_y\end{bmatrix}=\begin{bmatrix}e_k m_k\Omega^2\cos(\Omega t+\varphi_k)\\ e_k m_k\Omega^2\sin(\Omega t+\varphi_k)\end{bmatrix}.\tag{8}$$

In the equation, f_x and f_y represent the components of the unbalance force at node k in the x- and y-directions, respectively, while φ_k denotes the initial phase of the unbalance

force. Based on the measured imbalance of the high-pressure rotor in the original gas turbine, the eccentric distances of unbalance at AMB1 and AMB2 are set as e_k= 0.134 mm, with their phase angles φ_k being 43.5°. For other rigid disks, e_k = 0.1 mm, and the phase angles are 21.2°, 33.4°, and 11.5°, respectively.

For the modeling of gravity in flexible rotor systems, the gravitational force acting at node k_1, corresponding to the rigid disk, is expressed as

$$F_m^{k_1} = -m_d^{k_1} * g. \tag{9}$$

where $m_d^{k_1}$ is the mass of the rigid disk at node k_1, and g is the gravitational acceleration. For the gravitational force at node k_2, where no rigid disk is present, it can be expressed in terms of the rotor material density as

$$F_m^{k_2} = \pi\rho l^{k_2} g\left(r_o^2 - r_i^2\right), \tag{10}$$

where ρ represents the material density, l^{k_2} denotes the calculated length of the rotor at node k_2, and r_o and r_i represent the outer and inner radii of the rotor, respectively.